

Nonuniversal transition to condensate formation in two-dimensional turbulence

Moritz Linkmann[†], Manuel Hohmann, Bruno Eckhardt[‡]

Fachbereich Physik, Philipps-University of Marburg, D-35032 Marburg, Germany

(Received xx; revised xx; accepted xx)

The occurrence of system-scale coherent structures, so-called condensates, is a well-known phenomenon in two-dimensional turbulence. Here, the transition to condensate formation is investigated as a function of the magnitude of the force and for different types of forcing. Random forces with constant mean energy input lead to a supercritical transition, while forcing through a small-scale linear instability results in a subcritical transition with bistability and hysteresis. That is, the transition to condensate formation in two-dimensional turbulence is nonuniversal. For the supercritical case we quantify the effect of large-scale friction on the value of the critical exponent and the location of the critical point.

1. Introduction

Two-dimensional (2d) and quasi-2d flows occur at macro- and mesoscale in a variety of physical systems. Examples include stratified layers in Earth's atmosphere and the ocean (Vallis 2006), soap films and more recently also dense bacterial suspensions, where the collective motion of microswimmers induces patterns of mesoscale vortices (Dombrowski *et al.* 2004; Dunkel *et al.* 2013; Gachelin *et al.* 2014). A characteristic feature of 2d turbulence is the occurrence of an inverse energy cascade (Kraichnan 1967; Boffetta & Ecke 2014), whereby kinetic energy is transferred from small to large scales. In confined systems, this self-organisation can result in the formation of large-scale coherent structures (Kraichnan 1967; Hossain *et al.* 1983; Sommeria 1993; Smith & Yakhot 1993), so-called condensates (Smith & Yakhot 1993), which emerge in different forms depending on geometry and boundary conditions, e.g. as vortex dipoles or jets (Bouchet & Simonnet 2009; Frishman *et al.* 2017).

The inverse energy cascade in 2d turbulence is connected with an additional inviscid conservation law, that of enstrophy. However, inverse cascades and thus condensates are not specific to 2d phenomena. They occur whenever fluctuations in one spatial coordinate are suppressed, as is the case in thin fluid layers (Xia *et al.* 2009; Celani *et al.* 2010; Musacchio & Boffetta 2017), or, for instance, in presence of rapid rotation (Rubio *et al.* 2014; Deusebio *et al.* 2014; Gallet 2015), stratification (Sozza *et al.* 2015) or both (Marino *et al.* 2013), and in presence of a strong uniform magnetic field (Gallet & Doering 2015) for weakly conducting flows. Another, fully three-dimensional (3d), mechanism that leads to inverse energy transfer is breaking of mirror-symmetry (Waleffe 1993; Biferale *et al.* 2012). In magnetohydrodynamic turbulence the latter can result in the formation of magnetic condensates through large-scale dynamo action or the inverse cascade of magnetic helicity (Frisch *et al.* 1975; Pouquet *et al.* 1976).

There is thus a variety of systems that potentially allow mean energy transfer from

[†] Email address for correspondence: moritz.linkmann@physik.uni-marburg.de

[‡] Deceased on the 7th of August 2019.

small to large scales, which leads to a variety of possible transitions to spectral self-organisation and large-scale pattern formation, the nature of which depends on the details of the system, and smooth, supercritical and subcritical transitions between non-equilibrium statistically steady states have been observed. In 3d rotating domains for example, the nature of the transition between forward and inverse energy transfer with respect to the rotation rate depends on the mechanism by which the condensate saturates (Seshasayanan & Alexakis 2018). The two saturation scenarios are: (i) saturation by viscous effects as in 2d, where the condensate becomes sufficiently energetic for the upscale flux to be balanced by viscous dissipation, or (ii) saturation by local cancellation of the rotation rate by the counter-rotating vortex that forms part of the condensate (Alexakis 2015). In case (i) the transition is supercritical (Seshasayanan & Alexakis 2018), and in (ii) it is subcritical (Alexakis 2015; Yokoyama & Takaoka 2017; Seshasayanan & Alexakis 2018), showing bistability and hysteresis (Yokoyama & Takaoka 2017). Similar results have been obtained if the magnitude of the forcing is used as a control parameter at a fixed value of the rotation rate (Yokoyama & Takaoka 2017), with random and static forcing both resulting in a subcritical transition. The latter was interpreted as evidence in support of universality. Hysteretic transitions and bistable scenarios also occur in thin layers as a function of the layer thickness (van Kan & Alexakis 2019). Subcriticality in the transition to condensate formation in rapidly rotating Rayleigh-Bénard convection has been connected with non-local energy transfer from the driven scales into the condensate due to persistent phase correlations (Favier *et al.* 2019).

In summary, transitions in cascade directions from direct to inverse and vice versa have received considerable attention in recent years, Alexakis & Biferale (2018) provide a comprehensive overview thereof. In contrast, transitions to condensate formation in purely 2d turbulence have been studied only in the context of active matter, where spatiotemporal chaos and classical 2d turbulence with a condensate are connected by a subcritical transition (Linkmann *et al.* 2019*a,b*). Here, we extend this work and focus on the transition to condensate formation in two-dimensional turbulence as a function of the intensity the driving and in presence of large-scale friction. Conceptually, the 2d geometry differs substantially from thin layers or rapidly rotating 3d domains, as the energy transfer is now purely inverse. That is, the transition investigated here does not occur between two non-equilibrium statistically steady states with different multiscale dynamics. Instead, in 2d one state has multiscale dynamics and the other is a spatiotemporally chaotic state concentrated at the driven scales. Hence the transition in 2d is towards and away from multiscale dynamics, not between different types of such. By means of direct numerical simulations we show that the nature of the transition depends on the type of driving: It is supercritical for random forcing and subcritical if the driving is given by a small-scale linear instability. In the former case we also explore the effect of large-scale friction on the location of the critical point and the value of the critical exponent.

2. Numerical details

We consider the 2d Navier-Stokes equations for incompressible flow in a square domain V embedded in the xy -plane with periodic boundary conditions. In this case, the Navier-Stokes equations can be written in vorticity form

$$\partial_t \omega + (\omega \cdot \nabla) \mathbf{u} = -\alpha \omega + \nu \Delta \omega + (\nabla \times \mathbf{f})_z, \quad (2.1)$$

where $\mathbf{u} = (u_x(x, y), u_y(x, y), 0)$ is the velocity field per unit mass, ω the non-vanishing component of its vorticity $\nabla \times \mathbf{u} = (0, 0, \omega)$, ν the kinematic viscosity, $\alpha \geq 0$ the Ekman

friction coefficient and \mathbf{f} a solenoidal body force. The subscripts x , y and z denote the respective components of a 3d vector field.

We carry out direct numerical simulations of Eq. (2.1) on $V = [0, 2\pi]^2$ using the standard pseudospectral method (Orszag 1969) for spatial discretization in conjunction with full dealiasing by truncation following the 2/3rds rule (Orszag 1971). The initial data consist of random, Gaussian distributed vorticity fields. Owing to the focus on condensate formation and its dependence on large-scale friction, the friction coefficient α was small or set to zero in some of the simulations. In the latter case the condensate saturates on a viscous time scale (Chan *et al.* 2012; Linkmann *et al.* 2019b) with the consequence that the simulations need to be evolved for a long time in order to obtain statistically stationary states. Similarly long transients occur for low values of α . As such, it was necessary to compromise on resolution, and the simulations were run using $256^2 - 512^2$ grid points.

In order to study transitions to condensate formation, we conduct a parameter study for a stochastic, Gaussian distributed and δ -in-time correlated force \mathbf{f}_s that is applied at scales corresponding to a wavenumber interval $[k_{\min}, k_{\max}]$, and compare the results with those obtained with a forcing that is linear in the velocity field (Linkmann *et al.* 2019a,b), i.e.

$$\hat{\mathbf{f}}_l(\mathbf{k}) = \nu_i k^2 \gamma_k \hat{\mathbf{u}}(\mathbf{k}) , \quad (2.2)$$

where γ_k is a spherically symmetric Galerkin projector

$$\gamma_k = \begin{cases} 1 & \text{for } k \in [k_{\min}, k_{\max}] , \\ 0 & \text{otherwise} . \end{cases} \quad (2.3)$$

Here $k = |\mathbf{k}|$, while $\hat{\cdot}$ denotes the Fourier transform and $\nu_i > 0$ an amplification factor, such that the driving occurs through a linear instability in the wavenumber interval $[k_{\min}, k_{\max}]$. For numerical stability an additional dissipation term $\tilde{\nu} \Delta \omega$ is used at small scales, i.e. at $k > k_{\min}$, where the parameter $\tilde{\nu} = (\nu_2 - \nu) > 0$ mimicks the effect of hyperviscosity. The linear forcing is inspired by single-equation models describing dense bacterial suspensions (Wensink *et al.* 2012; Słomka & Dunkel 2015; Linkmann *et al.* 2019a,b), where *active turbulence* occurs. The latter is a spatiotemporally chaotic state characterised by the formation of mesoscale vortices owing to the collective effects of the microswimmers. These vortices occur in a narrow band of length scales, and can be described through a linear instability in the wavenumber interval $[k_{\min}, k_{\max}]$ (Wensink *et al.* 2012; Słomka & Dunkel 2015; Linkmann *et al.* 2019b). For both \mathbf{f}_s and \mathbf{f}_l , statistically stationary states are eventually reached, where the spatiotemporally averaged energy dissipation, ε , balances the spatiotemporally averaged energy input, ε_{IN} ,

$$\varepsilon := \langle \varepsilon(t) \rangle_t = \nu \langle \omega^2 \rangle_{V,t} + \alpha \langle |\mathbf{u}|^2 \rangle_{V,t} = \langle \mathbf{f} \cdot \mathbf{u} \rangle_{V,t} = \langle \varepsilon_{\text{IN}}(t) \rangle_t =: \varepsilon_{\text{IN}} , \quad (2.4)$$

with $\langle \cdot \rangle_{V,t} = \langle \langle \cdot \rangle_V \rangle_t$ denoting the combined spatial and temporal average. For Gaussian-distributed and $\delta(t)$ -correlated random forcing, ε_{IN} is known *a priori* (Novikov 1965)

$$\varepsilon_{\text{IN}s} = \langle \mathbf{f}_s \cdot \mathbf{u} \rangle_{V,t} = \frac{F^2}{2} , \quad (2.5)$$

where $F = \langle |\mathbf{f}_s| \rangle_{V,t}$. That is, the energy input is a control parameter rather than an observable in simulations using \mathbf{f}_s . Details of the simulations are summarised in table 1.

For the linear forcing, the energy input is

$$\varepsilon_{\text{IN}l}(t) = 2(\nu_i - \nu) \int_{k_{\min}}^{k_{\max}} dk \, k^2 E(k, t) , \quad (2.6)$$

N	F	α	Re	Re_f	U	U_f	L	τ
256	0.08-0.23	0	21-11817	9.4 - 11.8	0.09 - 3.05	0.06 - 0.07	0.11 - 1.94	1.21 - 0.64
256	0.10-0.29	0.0005	19 - 10083	9.4 - 15.0	0.09 - 2.67	0.06 - 0.09	0.11 - 1.89	1.24 - 0.71
256	0.10-0.32	0.001	19 - 8719	9.4 - 16.8	0.09 - 2.36	0.06 - 0.10	0.11 - 1.85	1.24 - 0.78
256	0.10-0.32	0.005	17 - 3592	9.5 - 18.3	0.09 - 1.08	0.06 - 0.11	0.10 - 1.67	1.15 - 1.55
512	0.11	0	29.1	9.79	0.106	0.057	0.14	1.32
512	0.14	0	2321.5	10.14	0.627	0.059	1.85	2.95
512	0.23	0	12587.2	11.45	3.242	0.067	1.94	0.60

TABLE 1. Simulation details, where N is the number of grid points in each coordinate, F the magnitude of the force acting in the interval $[k_{\min}, k_{\max}]$ with $k_{\min} = 33$ and $k_{\max} = 40$ for all simulations, α the large-scale friction parameter, $\text{Re} = UL/\nu$ the Reynolds number with respect to the root-mean-square velocity U , the integral length scale $L = 2/U^2 \int_0^\infty dk E(k)/k$ and the kinematic viscosity ν . The latter was set to $\nu = 0.0005$ for all simulations. The Reynolds number at the driven scales is $\text{Re}_f = U_f L_f/\nu$, with $U_f = \left(\int_{k_{\min}}^{k_{\max}} dk E(k) \right)^{1/2}$ denoting the velocity at the driven scales and $L_f = 2\pi/(k_{\min} + k_{\max})$. The large-eddy turnover time is denoted by $\tau = L/U$, and $\eta = (\nu^3/\varepsilon)^{1/4}$.

where

$$E(k, t) = \frac{1}{2} \int_{|\mathbf{k}|=k} d\mathbf{k} |\hat{\mathbf{u}}(\mathbf{k}, t)|, \quad (2.7)$$

is the energy spectrum. Equation (2.1) with $\mathbf{f} = \mathbf{f}_l$ and the aforementioned enhanced small-scale damping has been solved numerically by Linkmann *et al.* (2019a,b) in the context of transitions to large-scale pattern formation in dense suspensions of active matter. Here, we compare our simulations listed in table 1 against the data of Linkmann *et al.* (2019a,b), which is summarised in table 2. All simulations are evolved for several thousand large-eddy turnover times $\tau = L/U$, where U is the root-mean-square velocity and $L = 2/U^2 \int_0^\infty dk E(k)/k$ the integral length scale, with $E(k) = \langle E(k, t) \rangle_t$.

3. Random forcing

Before reporting on the results from the parameter study varying F , we briefly discuss dynamical and statistical properties of the simulated flows using three example cases with $F = 0.11$, $F = 0.14$ and $F = 0.23$. Time series of the kinetic energy and visualisations of the vorticity field corresponding to these three cases are shown in Fig. 1. For $F = 0.23$ a condensate consisting of two counter-rotating vortices has formed. The remaining cases do not show large-scale structure formation.

Figure 2 presents energy spectra (left) and normalised fluxes (right) for $F = 0.11$, $F = 0.14$ and $F = 0.23$. A scaling range characterised by a scaling exponent of the energy spectrum close to the Kolmogorov-value $-5/3$ and a nearly wavenumber-independent flux only form at the largest value of F . For smaller F the flux tends to zero rapidly for $k < k_{\min}$, hence dissipation cannot be negligible in this wavenumber range. In all cases the maximum and minimum values of the normalised flux do not add up to unity, which indicates that a substantial amount of energy is dissipated directly in the driving range. Interestingly, for the intermediate F , the scaling exponent of the energy spectrum is still

N	$(\nu_i - \nu)/\nu$	$\tilde{\nu}/\nu$	k_{\min}	k_{\max}	Re	Re _f	U	L	τ
256	0.25 - 7.0	10.0	33	40	19 - 13677	14 - 21	0.29 - 7.77	0.07 - 1.92	0.24 - 2.29
1024	1.0	10.0	129	160	45	21	0.027	0.029	1.07
1024	2.0	10.0	129	160	226	20	0.041	0.094	2.29
1024	5.0	10.0	129	160	132914	15	1.17	1.93	1.65

TABLE 2. Parameters used in DNSs of the piecewise constant viscosity model and resulting observables (Linkmann *et al.* 2019a,b). The number of grid points in each coordinate is denoted by N , the viscosity by ν , and ν_i , k_{\min} , k_{\max} are the parameters in Eqs. (2.2)-(2.3). The Reynolds number $\text{Re} = UL/\nu$ is based on ν , the root-mean-square velocity U and the integral length scale $L = 2/U^2 \int_0^\infty dk E(k)/k$, with $\nu = 1.1 \times 10^{-3}$ for $N = 256$ and $\nu = 1.7 \times 10^{-5}$ for $N = 1024$. The parameter $\tilde{\nu} = (\nu_2 - \nu)$ is an additional dissipation term that mimicks the effect of hyperviscosity at $k > k_{\min}$. The large-scale friction parameter $\alpha = 0$ for all simulations. Averages in the statistically stationary state are computed from at least 1800 snapshots separated by one large-eddy turnover time $\tau = L/U$.

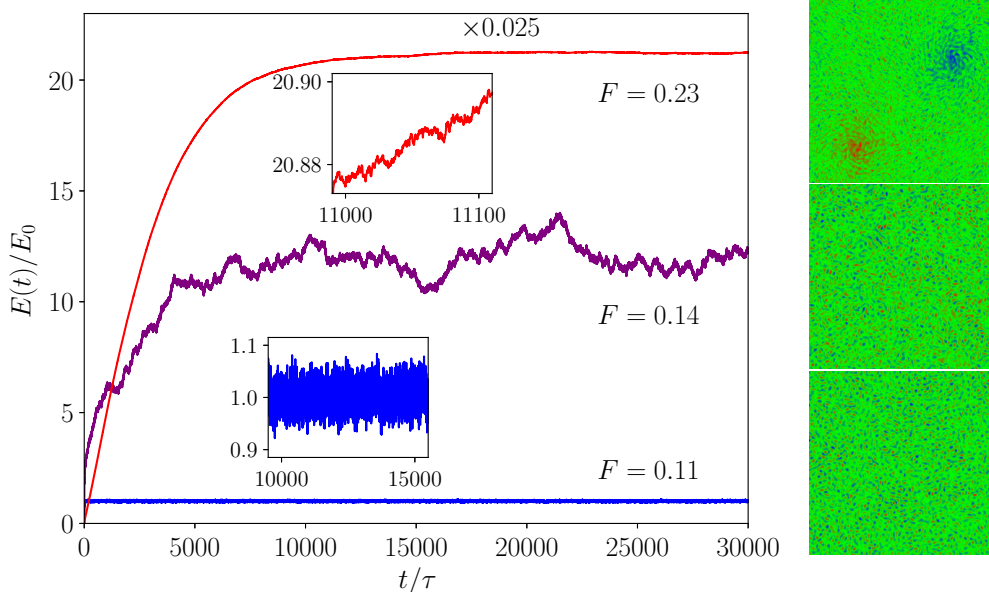


FIGURE 1. Left: Time series for $\alpha = 0$ and $F = 0.11$ (blue), $F = 0.14$ (purple) and $F = 0.23$ (red). The data has been normalised with respect to the time averaged energy for $F = 0.11$, E_0 , and the data for $F = 0.23$ has been further divided by a factor 40 for presentational purposes. Time is given in units of large-eddy turnover time τ . Right: Corresponding visualisations of the respective vorticity fields during statistically stationary evolution.

close but slightly larger than $-5/3$. For the smallest value of F the energy spectrum scales linearly with k for $k < 7$, indicative of energy equipartition among Fourier modes in this wavenumber range. A similar transition in the energy spectra in statistically stationary 2d turbulence occurs if the condensate is avoided through a strong drag term (Tsang & Young 2009), in the sense that the extent of the $-5/3$ scaling range decreases with increasing large-scale friction and a power law with positive exponent appears at

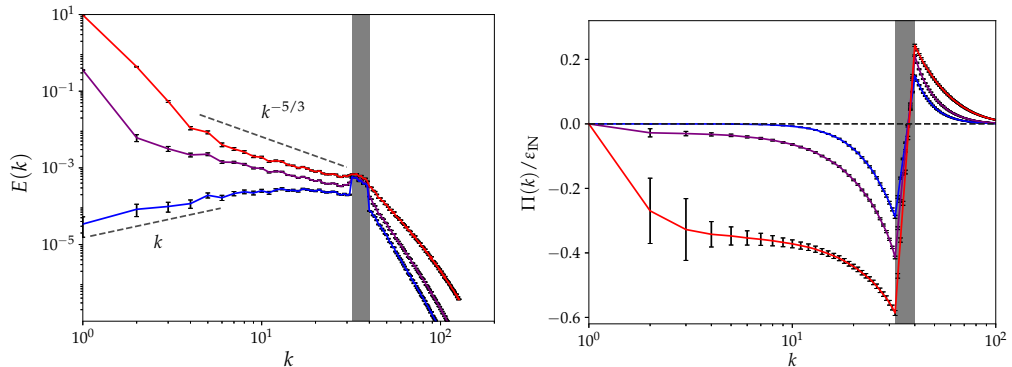


FIGURE 2. Energy spectra (left) and normalised fluxes (right) for $\alpha = 0$ and $F = 0.11$ (red), $F = 0.14$ (purple) and $F = 0.23$ (blue) for higher-resolved data in table 1. The grey-shaded area indicates the driving range. The error bars indicate the standard error calculated from statistically independent samples.

low wavenumbers. However, as a drag term alters the scale-by-scale energy balance, it breaks the zero-flux equilibrium condition that underlies linear scaling in 2d, the low-wavenumber scaling in presence of drag is expected to differ from the absolute equilibrium scaling observed here for $\alpha = 0$. Indeed, in the former case the spectra are much steeper (Tsang & Young 2009).

Condensates are known to affect inertial-range physics in terms of the properties of the third-order structure function (Xia *et al.* 2008) and the scaling of the energy spectrum in the inertial range of scales (Chertkov *et al.* 2007). The spectral slopes observed here for the random forcing case and in presence of a condensate are similar to those reported by Linkmann *et al.* (2019b) for the linearly forced case, hence the details of the small-scale forcing do not affect the spectral exponent. Deviations of the spectral exponent from the Kolmogorov value occur in a variety of turbulent systems. For a modified version of the Kuramoto-Sivashinski equation that allowed systematic deviations from inertial transfer, Bratanov *et al.* (2013) showed by semi-analytical and numerical means that nonuniversal power laws arise in spectral intervals where the ratio of linear and non-linear time scales is wavenumber-independent. As strong condensates result in a significant contribution of linear terms to the dynamics, a similar analysis could potentially lead to further insights on the nonuniversal scaling exponents in 2d turbulence.

4. Nonuniversal transitions

The transition to condensate formation in 2d turbulence as a function of the energy input has so far only been investigated for a single-equation model of active matter (Linkmann *et al.* 2019a,b). Here, we now study the transition for a different kind of forcing and in presence of large-scale friction, as condensates also occur in presence of drag (Danilov & Gurarie 2001; Tsang & Young 2009).

The left panel of Fig. 3 presents the amplitude of the lowest Fourier mode, i.e. the square root of the average energy at the largest scale, $A_1 = \sqrt{E(k)_{k=1}}$, as a function of F from the parameter study for the random, Gaussian distributed and $\delta(t)$ -correlated forcing. Three main observations can be made from the left panel of the figure. First, there is a clear transition point, below which $A_1 \simeq 0$ and above which A_1 grows with increasing F , indicating the formation of a condensate. Second, the data appears to be continuous at the critical point F_c with a possibly discontinuous first derivative. The

critical point is approached from above by a power law

$$A_1 \sim (F - F_c)^\gamma, \quad (4.1)$$

where $F_c = F_c(\alpha)$ and $\gamma = \gamma(\alpha)$ depend on the value of the large-scale friction coefficient. For $\alpha = 0$ the functional form $A_1(F)$ corresponds to the upper branch of the normal form of a supercritical pitchfork bifurcation, that is $\gamma = 1/2$, even though the stochastic nature of the system makes comparisons to concepts from dynamical systems theory difficult. A least-squares fit of A_1 against F places the critical point at $F_c = 0.135$. For $\alpha = 0.0005$ we have $F_c = 0.137$ and $\gamma = 0.685$, $\alpha = 0.001$ results in $F_c = 0.137$ and $\gamma = 0.8$ and $\alpha = 0.005$ corresponds to $F_c = 0.143$ and $\gamma = 1$. That is, while the approach to the critical point is strongly dependent on the level of large-scale friction, the location of the critical point varies little. Third, for $F \gg F_c$ the amplitude A_1 grows linearly with F in all cases. Equivalently, $E(k)_{k=1}$ grows linearly with ε_{IN} , which is expected for a sizeable condensate as most of the dissipation should then take place at the largest scales

$$\varepsilon_{\text{IN}} = \varepsilon = 2\nu \int_0^\infty dk k^2 E(k) + \alpha \int_0^\infty dk E(k) \approx (2\nu + \alpha) E(k)_{|k=1} \delta k, \quad (4.2)$$

where δk is the grid spacing in Fourier space. The same argument suggests that one can expect the linear scaling $A_1 \sim (F - F_c)$ observed for $\alpha = 0.001$ asymptotically for strong friction.

The type of transition is very different if the driving occurs through a small-scale linear instability. The right panel of Fig. 3 shows A_1 from the data of Linkmann *et al.* (2019a,b) as a function of ν_i for the linear forcing specified in Eq. (2.2). In contrast to the randomly forced case, the transition is now subcritical (Linkmann *et al.* 2019a,b) as evidenced by a discontinuity in the data and the clearly visible hysteresis loop. As the hysteresis loop is small, one may expect that the transitions happen at comparable values of a forcing-scale Reynolds number $\text{Re}_f = U_f L_f / \nu$, where L_f is a length scale that corresponds to the middle wavenumber in the driven range, $L_f = 2\pi / (k_{\min} + k_{\max})$, and U_f is the rms velocity in that range of scales

$$U_f = \left(\int_{k_{\min}}^{k_{\max}} dk E(k) \right)^{1/2}. \quad (4.3)$$

This is indeed the case, the transition occurs at $\text{Re}_f \approx 15 - 20$ in the subcritical case (Linkmann *et al.* 2019a) and at $\text{Re}_f \approx 10$ in the supercritical case studied here.

5. Conclusions

We here study the formation of the condensate as a function of the type and amplitude of the forcing. Direct numerical simulations show that the condensate does not appear gradually but in a phase transition. For prescribed energy dissipation the transition is second order, and both the critical point and the critical exponent depend on the value of the large-scale friction coefficient. In this context, we point out that ε does not depend on α for the random, $\delta(t)$ -correlated forcing used here, as is the case for time-independent forcing such as Kolmogorov flow (Tsang & Young 2009). However, a series of test simulations using time-independent forcing led to similar results (Musacchio & Boffetta, private communication). When the forcing is due to a small-scale instability as inspired by continuum models of active matter, the transition is first order (Linkmann *et al.* 2019a,b). The phase transitions separate two markedly different types of 2d dynamics: in turbulence with a condensate, energy input is predominantly balanced by dissipation in

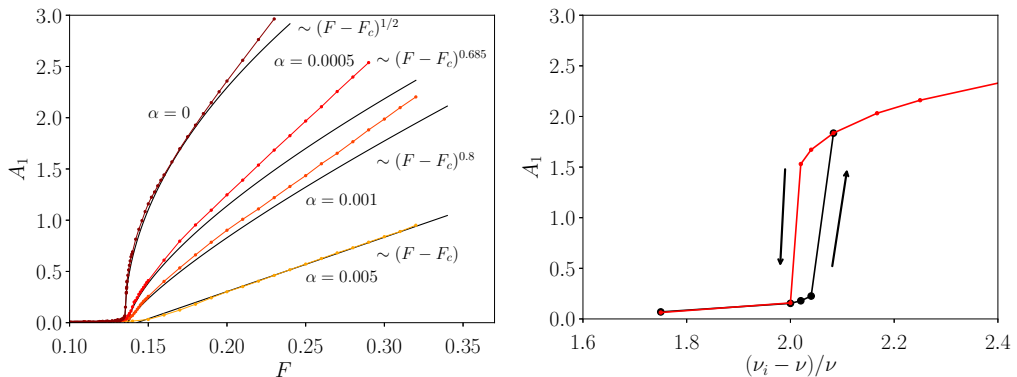


FIGURE 3. Amplitude of the Fourier mode at the largest scale, $A_1 = \sqrt{E(k)_{k=1}}$, as a function of F for random forcing (left) and ν_i for linear forcing (right).

the condensate and intermediate scales follow an inertial cascade; without a condensate dissipation is spread over the intermediate scales and the properties of the energy transfer are noticeably different and nonuniversal.

In summary, the transition to condensate formation in 2d turbulence is nonuniversal in the sense that (i) the type of transition depends on the type of forcing, and (ii) the details of the transition for a given type of forcing depend on other system parameters such as large-scale friction. The presence of these nonuniversalities naturally motivate questions concerning their origin. Results from rapidly rotating RBC (Favier *et al.* 2019) suggest that the hysteretic transition in the linearly forced case may be related to persistent phase correlations between the driven scales and the condensate. Random forcing precludes such a scenario. Further questions concern the theoretical predictions on the dependence of the critical exponent γ on the level of large-scale friction. The value $\gamma = 1$ is plausible for strong linear damping by the same argument that predicted a linear dependence of the energy in the condensate on the energy input.

Acknowledgements

Bruno Eckhardt sadly passed away before the manuscript was written. We hope to have summarised the collaborative work according to his standards, and any shortcomings should be attributed to ML. We will remember him as an outstanding scientist, thoughtful supervisor and inspiring role model. ML thanks Guido Boffetta and Stefano Musacchio for helpful discussions.

REFERENCES

- ALEXAKIS, A. 2015 Rotating Taylor-Green flow. *J. Fluid Mech.* **769**, 46–78.
- ALEXAKIS, A. & BIFERALE, L. 2018 Cascades and transitions in turbulent flows. *Phys. Reports* **767–769**, 1–101.
- BIFERALE, L., MUSACCHIO, S. & TOSCHI, F. 2012 Inverse energy cascade in three-dimensional isotropic turbulence. *Phys. Rev. Lett.* **108**, 164501.
- BOFFETTA, G. & ECKE, R. E. 2014 Two-Dimensional Turbulence. *Annu. Rev. Fluid Mech.* **44**, 427–451.
- BOUCHET, F. & SIMONNET, E. 2009 Random Changes of Flow Topology in Two-Dimensional and Geophysical Turbulence. *Phys. Rev. Lett.* **102**, 094504.
- BRATANOV, V., JENKO, F., HATCH, D. R. & WILCZEK, M. 2013 Nonuniversal power-law spectra in turbulent systems. *Phys. Rev. Lett.* **111**, 075001.

- CELANI, A., MUSACCHIO, S. & VINCENZI, D. 2010 Turbulence in More Than Two and Less Than Three Dimensions. *Phys. Rev. Lett.* **104**, 184506.
- CHAN, C., MITRA, D. & BRANDENBURG, A. 2012 Dynamics of saturated energy condensation in two-dimensional turbulence. *Phys. Rev. E* **85**, 036315.
- CHERTKOV, M., CONNAUGHTON, C., KOLOKOLOV, I. & LEBEDEV, V. 2007 Dynamics of Energy Condensation in Two-Dimensional Turbulence. *Phys. Rev. Lett.* **99**, 084501.
- DANILOV, S. & GURARIE, D. 2001 Forced two-dimensional turbulence in spectral and physical space. *Phys. Rev. E* **63**, 061208.
- DEUSEBIO, E., BOFFETTA, G., LINDBORG, E. & MUSACCHIO, S. 2014 Dimensional transition in rotating turbulence. *Phys. Rev. E* **90**, 023005.
- DOMBROWSKI, C., CISNEROS, L., CHATKAEW, S., GOLDSTEIN, R. E. & KESSLER, J. O. 2004 Self-Concentration and Large-Scale Coherence in Bacterial Dynamics. *Phys. Rev. Lett.* **93**, 098103.
- DUNKEL, J., HEIDENREICH, S., DRESCHER, K., WENSINK, H. H., BÄR, M. & GOLDSTEIN, R. E. 2013 Fluid dynamics of bacterial turbulence. *Phys. Rev. Lett.* **110**, 228102.
- FAVIER, B., GUERVILLY, C. & KNOBLOCH, E. 2019 Subcritical turbulent condensate in rapidly rotating Rayleigh-Bénard convection. *J. Fluid Mech.* **864**, R1.
- FRISCH, U., POUQUET, A., LÉORAT, J. & MAZURE, A. 1975 Possibility of an inverse cascade of magnetic helicity in magnetohydrodynamic turbulence. *J. Fluid Mech.* **68**, 769–778.
- FRISHMAN, A., LAURIE, J. & FALKOVICH, G. 2017 Jets or vortices - what flows are generated by an inverse turbulent cascade? *Phys. Rev. Fluids* **2**, 032602.
- GACHELIN, J., ROUSSELET, A., LINDNER, A. & CLEMENT, E. 2014 Collective motion in an active suspension of *escherichia coli* bacteria. *New Journal of Physics* **16**, 025003.
- GALLET, B. 2015 Exact two-dimensionalization of rapidly rotating large Reynolds-number flows. *J. Fluid Mech.* **783**, 412–447.
- GALLET, B. & DOERING, C. R. 2015 Exact two-dimensionalization of low-magnetic-Reynolds-number flows subject to a strong magnetic field. *J. Fluid Mech.* **773**, 154–177.
- HOSSAIN, M., MATTHAEUS, W. H. & MONTGOMERY, D. 1983 Long-time states of inverse cascades in the presence of a maximum length scale. *J. Plasma Physics* **30**, 479493.
- VAN KAN, A. & ALEXAKIS, A. 2019 Condensates in thin layer turbulence. *J. Fluid Mech.* **864**, 490–518.
- KRAICHNAN, R. H. 1967 Inertial ranges in twodimensional turbulence. *Phys. Fluids* **10**, 1417–1423.
- LINKMANN, M., BOFFETTA, G., MARCHETTI, M. C. & ECKHARDT, B. 2019a Phase Transition to Large Scale Coherent Structures in Two-Dimensional Active Matter Turbulence. *Phys. Rev. Lett.* **122**, 214503.
- LINKMANN, M., MARCHETTI, M. C., BOFFETTA, G. & ECKHARDT, B. 2019b Condensate formation and multiscale dynamics in two-dimensional active suspensions. *arXiv:1905.06267*.
- MARINO, R., MININNI, P. D., ROSENBERG, D. & POUQUET, A. 2013 Inverse cascades in rotating stratified turbulence: fast growth of large scales. *Europhys. Lett.* **102**, 44006.
- MUSACCHIO, S. & BOFFETTA, G. 2017 Split energy cascade in turbulent thin fluid layers. *Phys. Fluids* **29**, 111106.
- NOVIKOV, E. A. 1965 Functionals and the random-force method in turbulence theory. *Soviet Physics JETP* **20**, 1290–1294.
- ORSZAG, S. A. 1969 Numerical methods for the simulation of turbulence. *Phys. Fluids* **12**, II–250–II–257.
- ORSZAG, S. A. 1971 On the Elimination of Aliasing in Finite-Difference Schemes by Filtering High-Wavenumber Components. *J. Atmos. Sci.* **28**, 1074.
- POUQUET, A., FRISCH, U. & LÉORAT, J. 1976 Strong MHD helical turbulence and the nonlinear dynamo effect. *J. Fluid Mech.* **77**, 321–354.
- RUBIO, A. M., JULIEN, K., KNOBLOCH, E. & WEISS, J. B. 2014 Upscale Energy Transfer in Three-Dimensional Rapidly Rotating Turbulent Convection. *Phys. Rev. Lett.* **112**, 144501.
- SESHASAYANAN, K. & ALEXAKIS, A. 2018 Condensates in rotating turbulent flows. *J. Fluid Mech.* **841**, 434–462.
- SŁOMKA, J. & DUNKEL, J. 2015 Generalized Navier-Stokes equations for active suspensions. *Eur. Phys. J. Spec. Top.* **224**, 1349.

- SMITH, L. M. & YAKHOT, V. 1993 Bose condensation and small-scale structure generation in a random force driven 2D turbulence. *Phys. Rev. Lett.* **71**, 352–355.
- SOMMERIA, J. 1993 Experimental study of the two-dimensional inverse energy cascade in a square box. *J. Fluid Mech.* **170**, 139–168.
- SOZZA, A., BOFFETTA, G., MURATORE-GINANNESCHI, P. & MUSACCHIO, S. 2015 Dimensional transition of energy cascades in stably stratified forced thin fluid layers. *Phys. Fluids* **27**, 035112.
- TSANG, Y.-K. & YOUNG, W. R. 2009 Forced-dissipative two-dimensional turbulence: A scaling regime controlled by drag. *Phys. Rev. E* **79**, 045308(R).
- VALLIS, G. K. 2006 *Atmospheric and Oceanic Fluid Dynamics*. Cambridge: Cambridge University Press.
- WALEFFE, F. 1993 Inertial transfers in the helical decomposition. *Phys. Fluids A* **5**, 677–685.
- WENSINK, H. H., DUNKEL, J., HEIDENREICH, S., DRESCHER, K., GOLDSTEIN, R. E., LÖWEN, H. & YEOMANS, J. M. 2012 Meso-scale turbulence in living fluids. *Proc. Natl. Acad. Sci.* **109**, 14308–14313.
- XIA, H., PUNZMANN, H., FALKOVICH, G. & SHATS, M. 2008 Turbulence-condensate interaction in two dimensions. *Phys. Rev. Lett.* **101**, 194504.
- XIA, H., SHATS, M. & FALKOVICH, G. 2009 Spectrally condensed turbulence in thin layers. *Physics of Fluids* **21** (12), 125101.
- YOKOYAMA, N. & TAKAOKA, M. 2017 Hysteretic transitions between quasi-two-dimensional flow and three-dimensional flow in forced rotating turbulence. *Phys. Rev. Fluids* **2**, 092602(R).